TLR7 Is Expressed by Support Cells, but Not Sensory Neurons, in Ganglia

Becky J. Proskocil
Oregon Health & Science University
Karol Wai
Oregon Health & Science University
Katherine M. Lebold
Oregon Health & Science University
Mason Norgard
Oregon Health & Science University
Katherine A Michaelis
Oregon Health & Science University
Daniel L. Marks
Oregon Health & Science University
Allison D. Fryer
Oregon Health & Science University
David B. Jacoby
Oregon Health & Science University
Matthew Georgenson Drake (drakem@ohsu.edu)
Division of Pulmonary and Critical Care Medicine, Oregon Health & Science University, Portland, OR 97239 https://orcid.org/0000-0001-5476-0361

Research

Keywords: Dorsal root ganglia, Iba1 (ionized calcium binding adaptor molecule 1), Influenza 1, Sensory nerve, TLR7 (Toll-like receptor 7), Vagal ganglia

Posted Date: January 5th, 2021

DOI: https://doi.org/10.21203/rs.3.rs-136876/v1

Abstract

Background: Toll like receptor 7 (TLR7) is an innate immune receptor that detects viral single-stranded RNA and triggers production of proinflammatory cytokines and type 1 interferons in immune cells. TLR7 agonists also modulate sensory nerve function by increasing neuronal excitability, although studies are conflicting whether sensory neurons specifically express TLR7. This uncertainty has confounded development of a mechanistic understanding of TLR7 function in nervous tissues.

Methods: TLR7 expression was tested using in situ hybridization with species-specific RNA probes in vagal and dorsal root sensory ganglia in wild-type and TLR7 knockout mice, and in guinea pigs. In situ labeling was compared to immunohistochemistry using TLR7 antibody probes. Pulmonary afferent neurons in vagal ganglia were also specifically tested since respiratory viruses are a common TLR7 ligand. Guinea pig vagal afferents were labeled by intranasal instillation of wheat germ agglutinin, isolated using flow cytometry and analyzed for TLR7 by RT-PCR. The effects of influenza A infection on TLR7 expression in sensory ganglia and in spleen were also assessed.

Results: In situ probes detected TLR7 in the spleens and in small support cells adjacent to sensory neurons in dorsal root and vagal ganglia in wild type mice and guinea pig, but not in TLR7 KO mice. TLR7 was co-expressed with the macrophage and satellite glial cell marker Iba1, but was absent in sensory nerves in vagal and dorsal root ganglia in both mice and guinea pigs. In contrast, a TLR7 antibody labeled small and medium-sized neurons in wild-type and TLR7 KO mice in a TLR7-independent manner. Wheat germ agglutinin-positive cells sorted by flow cytometry expressed both TLR7 and Iba1, indicating that TLR7-expressing support cells sort alongside neurons despite ganglia dissociation. Influenza A infection caused significant weight loss and upregulation of TLR7 in spleens, but not in vagal ganglia, in mice.

Conclusion: TLR7 is expressed by macrophages and satellite glial cells, but not neurons in sensory ganglia suggesting TLR7's neuromodulatory effects are mediated indirectly via activation of neuronally-associated support cells, not through activation of neurons directly. Our data also suggest TLR7's role in neuronal tissues is not primarily related to antiviral immunity.

Introduction

Toll like receptor 7 (TLR7) is pattern-recognition receptor that detects single-stranded viral RNA genomes and triggers an innate immune response [1]. Numerous inflammatory cells express TLR7, including T cells [2], B cells [3], eosinophils [4], and cells of the mononuclear phagocyte system such as macrophages [5–8] and monocytes [6]. In these cells, endosomal-bound viral RNA activates TLR7, which initiates a Myd88-dependent signal transduction pathway leading to the secretion of antiviral type I interferons and proinflammatory cytokines that are essential for antiviral immunity [9].

Recently, non-canonical roles for TLR7 in both the central and peripheral nervous system have also been reported. In the central nervous system, intrathecal injection of TLR7 agonists caused axonal injury and neuronal cell death in mice *in vivo* [10, 11] and reduced dendrite growth in cultured mouse cortical neurons *in vitro* [12], suggesting TLR7 influences cortical neurogenesis. Intradermal injection of TLR7 agonists also potentiated sensation of pain and itch in mice [13–15], suggesting TLR7 also has neuromodulatory effects on peripheral sensory nerve function. Whether these effects are due to direct activation of neurons or mediated indirectly by second messengers released from TLR7-expressing support cells in ganglia, such as satellite glial cells and resident macrophages, is controversial. Previous studies reported conflicting results regarding TLR7 expression in ganglia, with some showing neuronal TLR7 expression using commercially available TLR7 antibodies, while others reported either the presence or absence of neuronal TLR7 RNA expression using RT-PCR [13–18]. These discordant findings have complicated efforts to develop a mechanistic understanding of TLR7 function in nervous tissues.

Our laboratory has been interested in interactions between TLR7 and peripheral nerves in the lungs given that RNA respiratory viruses potentiate nerve-mediated bronchoconstriction [19–23] and are a common trigger for asthma exacerbations in humans [24]. Thus, in previous studies we tested whether the imidazoquinoline TLR7 agonists imiquimod (R837) and gardiquimod (R848) acutely increased nerve-mediated bronchoconstriction. On the contrary, we found that R837 and R848 paradoxically relaxed guinea pig airway *in vivo* and human airways *ex vivo* within minutes in part via production of nitric oxide [25, 26], suggesting TLR7 agonists have therapeutic potential as a novel class of bronchodilators. Based on this unexpected finding and since previously reports were contradictory regarding TLR7 expression by sensory nerves, we sought to characterize TLR7 expression within vagal ganglia, which supply sensory innervation to the lungs, using in situ hybridization. RNA probe specificity was validated in TLR7 knockout tissues. We compared findings in vagal ganglia to non-pulmonary sensory nerves within dorsal root ganglia. Results from in situ experiments were compared with immunohistochemistry using two commonly-cited TLR7 antibodies from different commercial sources. Furthermore, we tested whether influenza A infection induces TLR7 expression affects TLR7 RNA expression in sensory nerve ganglia and whether TLR7 agonists induce nitric oxide neurons and in ganglia support cells.

Methods

Animals. Wild type C57BL/6J and TLR7 knock out (B6.129S1-*Tlr7*^{tm1Flv}/J) mice were purchased from The Jackson Laboratory (Bar Harbor, ME) and were 11–18 weeks of age at the time of experimentation. Adult, female Hartley guinea pigs were purchased from Charles River Laboratories (Wilmington, MA) and were 350–500 g at the time of experimentation. All animals were housed in filtered air rooms, given *ad libitum* access to food and water, and exposed to 12-hour light/dark cycle. Animals were treated in accordance with standards established by the United States Animal Welfare Act set forth by National Institutes of Health guidelines. The Institutional Animal Care and Use Committee at Oregon Health & Science University approved all experimental protocols.

In situ hybridization. Mice and guinea pigs were euthanized with an overdose of pentobarbital. Animals were perfused with PBS and tissues were dissected and fixed in 10% neutral buffered formalin for 16–24 h at room temperature (RT). Paraffin sections (5 μm) and tissue blocks were stored at 4 °C in a desiccator. The RNAscope in situ hybridization assay (Advanced Cell Diagnostics, San Francisco, CA) was followed per kit instructions with a 15 min incubation in the RNAscope Target Retrieval reagent and a 30 min incubation in the RNAscope Protease Plus reagent (Advanced Cell Diagnostics, 322330). RNAscope probes (mouse TLR7 415411, mouse piptidylprolyl isomerase B (Ppib) positive control 313911, guinea pig TLR7 563131, guinea pig Ppib positive control 471531, dihyrdodipicolinate reductase (DapB) negative control 310043, Advanced Cell Diagnostics) were detected with the RNAscope 2.5 HD Detection Reagents-RED kit (Advanced Cell Diagnostics, 322360). Slides were counterstained with Gills Hematoxylin (1:1 with water, American MasterTech Scientific) and imaged on a Zeiss Apotome Microscope (Oberkochen, Germany).

For in situ hybridization on cultured nodose and jugular ganglia, ganglia were dissociated from naïve guinea pigs as previously described [27]. Cells were plated on laminin (Life Technologies, Frederick, MD) coated glass-bottom fluorodishes (World Precision Instruments, Saratoga, FL) and cultured in media consisting of 1:1 F12:DMEM media (Thermo Fisher Scientific, Waltham, MA), 100 U/ml penicillin, 100 μg/ml streptomycin, 10 μg/ml guinea pig transferrin (BP25445, FisherScientific), 100 ng/ml nerve growth factor 2.5S (NG009, Sigma-Aldrich, St. Louis, MO), and 20 μM camptothecin (Sigma-Aldrich, St. Louis, MO). After 4 days, cells were fixed and processed for RNAscope in situ hybridization following the Advanced Cell Diagnostics Technical Note for Cultured Adherent Cells. Cells were incubated with guinea pig-specific probes for TLR7 RNA (Advanced Cell Diagnostics, guinea pig TLR7 563131), and the probes were detected with the RNAscope 2.5 HD Detection Reagents-RED (Advanced Cell Diagnostics, 322360) kit. Cells were coverslipped and imaged on Nikon Eclipse Ci microscope (Tokyo, Japan) using an Andor Zyla camera at 100X (Nikon Plan Flour 1.3NA).

Immunohistochemistry. Wild type mice, TLR7 KO mice, and guinea pigs were euthanized with an overdose of pentobarbital and perfused with PBS. Dorsal root ganglia (DRG), vagal ganglia (containing the nodose and jugular ganglia) and spleens were collected for testing TLR7 in situ hybridization probes. Tissues were fixed in 10% neutral buffered formalin for 16–24 h at RT, then washed and prepared for paraffin sectioning. Slides were dewaxed with xylene and rehydrated with a decreasing series of alcohols to water.

For TLR7 immunohistochemistry, all slides were treated for 10 min in a 90 °C water bath with antigen unmasking solution (Vector Laboratories, Burlingame, CA) and then for 10 min in 3% hydrogen peroxide made in 4 °C methanol to block endogenous peroxidase. After washing, non-specific binding was blocked with 10% normal goat serum (Vector Laboratories) made in PBS containing 0.05% Tween-20 (PBST) for 1 h at RT. Slides were incubated overnight at 4 °C in a humidified chamber with either anti-TLR7 polyclonal antibody (1:1000, rabbit, Novus cat. # NBP2-24906.) or anti-TLR7 monoclonal antibody (1:250, rabbit, Abcam cat. # ab124928) made in blocking buffer. A serial section did not receive primary antibody to determine background signal. Slides were then washed, incubated for 1 h at RT with a biotinylated

secondary antibody (1:400, goat anti-rabbit, Vector Laboratories), and then 30 min with avidin biotin complex (Vector Laboratories). Slides were reacted with diaminobenzidine peroxidase (DAB, Vector Laboratories). Slides from TLR7 KO and wild type mice were reacted with DAB for the same duration. Slides were rinsed, counterstained with Gills Hematoxylin (1:1 with water, American MasterTech Scientific), mounted, and imaged on a Zeiss Apotome Microscope.

For immunohistochemistry following in situ hybridization, slides were incubated in 3% hydrogen peroxide made in water for 10 min at RT to quench any remaining peroxidase activity from the in situ hybridization assay and then rinsed in water and PBST. To detect ionized calcium binding adaptor molecule 1 (Iba1), a marker for macrophages/microglia, non-specific binding was blocked with 10% normal rabbit serum (Vector Laboratories) made in PBST for 1 h at RT, and then slides were incubated with an anti-Iba1 antibody (1:2500, goat polyclonal, Abcam 5076, Cambridge, United Kingdom) overnight in blocking buffer at 4 °C in a humidified chamber. Slides were then processed similarly as described above using a biotinylated rabbit anti-goat secondary antibody (1:400, Vector Laboratories). To detect protein gene product 9.5 (PGP 9.5), a pan-neuronal marker, non-specific binding was blocked with 10% normal goat serum (Vector Laboratories) made in PBST for 1 h at RT, and then slides were incubated with an anti-PGP 9.5 antibody (1:1000, rabbit polyclonal, Millipore AB1761-I, Burlington, MA) overnight in blocking buffer at 4 °C in a humidified chamber. A goat anti-rabbit IgG H + L Alexa Flour 647 secondary antibody (1:1000, Thermo Fisher Scientific) was used for fluorescence detection of the antibody (1 h at RT) and then slides were mounted with Vectashield (Vector Laboratories) containing 4',6-diamidino-2-phenylidndole (DAPI) to label nuclei. All slides were imaged on a Zeiss Apotome Microscope.

Wheat germ agglutinin (WGA) and flow cytometry. Guinea pigs were sedated with 15 mg/kg ketamine and 2.5 mg/kg xylazine (i.m.). WGA Alexa Fluor 555 (Thermo Fisher Scientific) was diluted in sterile PBS such that 250 μl containing 0.25 mg WGA was delivered to guinea pigs by intranasal administration. Three days after WGA administration, guinea pigs were euthanized with an overdose of pentobarbital. DRG and vagal ganglia were aseptically isolated taking care to avoid extended exposure to bright lights. Some ganglia were quickly checked for WGA uptake by viewing whole mounted ganglia at 10x on an Nikon Eclipse Ci microscope and imaged with an Andor Zyla sCMOS camera (Oxford Instruments, Abingdon, United Kingdom) (Fig. 3C). The nodose and jugular ganglia were separated and dissociated as previously described [27]. After dissociation, cells were resuspended in Hanks Balanced Salt solution (pH 7.4). Cells were sorted on BD Influx cell sorter (Becton Dickinson, Franklin Lakes, NJ), first by forward and side scatter to remove debris and then by pulse width to exclude cell doublets. Cells were then sorted by a 488 nm and 555 nm filter to gate for cells that had high 555 expression (WGA+), avoiding autofluorescent cells that had similar 488 and 555 signal. Gating parameters were established using cells isolated from guinea pigs that did not receive WGA. WGA + cells were sorted into a microcentrifuge tube and RNA was isolated using the RNeasy Micro kit (Qiagen, Germantown, MD).

Real time reverse transcriptase-polymerase chain reaction (real time RT-PCR). DRG, vagal ganglia, and brain were aseptically dissected. Guinea pig nodose and jugular ganglia were separated under a dissection microscope whereas mouse vagal ganglia, due to fusion of nodose and jugular ganglia in this

species, were processed as a single sample. RNA was isolated using the RNeasy Mini Kit (Qiagen). cDNA was generated from the RNA isolated from whole tissues or from WGA + cells using Superscript III Reverse Transcriptase (Thermo Fisher Scientific) and amplified using a Veriti 96-well Thermal Cycler (Applied Biosystems, Foster City, CA). Guinea pig TLR7 (5' GGCTGACCTTTGTGCTTCTC and 3' CACAATCACGTGGGTCTTTG) and Iba1 (5' GAGTTCCTCTGCGACCAGAA and 3' CCCCCAGCTTCTCCATCATC) primers were synthesized by Integrated DNA Technologies (Coralville, IA) and RNA expression was detected by real time RT-PCR (7500 Fast RT-PCR system, Applied Biosystems) using Sybr Green master mix (ThermoFisher). TLR7 and Iba1 PCR products were run on a 1.5% agarose gel and were determined to be the correct size (TLR7 = 222 base pairs and Iba1 = 148 base pairs). Bands were excised and DNA was isolated using the QIAquick Gel Extract kit (Qiagen). The DNA products were then sequenced by Sanger sequencing using an Applied Biosystems 3730xl 96-capilllary DNA analyzer to confirm the identity of the PCR product. Mouse TLR7 primers (cat. # Mm00446590_m1) and 18 s primers (cat. # 4352930E) were purchased from Applied Biosystems and amplified using TaqMan reagents by real time RT-PCR (7500 Fast RT-PCR system, Applied Biosystems). TLR7 expression was normalized using delta-delta CT.

Quantification of cellular nitric oxide. Neurons and support cells from dissociated ganglia were plated on laminin- (Life Technologies, Frederick, MD) coated glass-bottom fluorodishes (World Precision Instruments, Saratoga, FL) and cultured in media consisting of 1:1 F12:DMEM media (Thermo Fisher Scientific, Waltham, MA), 100 U/ml penicillin, 100 µg/ml streptomycin, 10 µg/ml guinea pig transferrin (BP25445, FisherScientific), 100 ng/ml nerve growth factor 2.5S (NG009, Sigma-Aldrich, St. Louis, MO), and 20 µM camptothecin (Sigma-Aldrich, St. Louis, MO) for 48 hours. Cells were loaded with a nitric oxide detecting fluorophore (FL2A, Strem Chemicals) for 30 minutes followed by treatment with TLR7 agonist R837 (10 µM, Invitrogen) for an additional 30 minutes. Some cells were pre-treated with TLR7 antagonist IRS661 (100 µM, Integrated DNA Technologies), TLR7 antagonist control oligomer (100 µM, Integrated DNA Technologies), or the nitric oxide synthase antagonist L-NAME (100 µM, Sigma). Cells were imaged on a Nikon spinning-disk confocal microscope (20X, 1.3 NA) and cellular fluorescence was quantified within individual cell bodies using Image J. Experimental replicates represent the average of 10–20 individual cells per experimental condition.

H1N1 infection. Wild type male mice were anesthetized with ketamine (45 mg/kg) and xylazine (8 mg/kg) i.p. and infected by intranasal administration (25 µL) of influenza A virus subtype H1N1 (ATCC A/PR/8/34 strain, $1e^5$ $TCID_{50}$ Units) or mock-infected with PBS vehicle. Viral stocks were grown in rhesus monkey kidney (RMK) cell monolayers, purified by sucrose density centrifugation, and titered in RMK cells. Mice were euthanized by an overdose of pentobarbital (150 mg/kg i.p.) 4 days later. The right lung and left vagal ganglia were flash frozen for RNA isolation using the RNeasy Mini Kit (Qiagen). The right vagal ganglia and spleen were fixed in 10% neutral buffered formalin at RT for 16–24 h for in situ hybridization assays.

Quantification of H1N1 RNA in lung. Primers for H1N1 were synthesized by Integrated DNA Technologies (Coralville, IA) as follows: 5' CATCCTGTTGTATATGAGGCCCAT and 3' TTCGCAGATGCGACGTCAGG. H1N1

titers from whole lung were quantified by real time RT-PCR (7500 Fast RT-PCR system, Applied Biosystems) using an H1N1 $TCID_{50}$ standard curve derived from serial dilutions of cDNA generated from the H1N1 viral stock solution. Samples were normalized for 18S cDNA.

Analysis of RNAscope in situ hybridization. Images of H1N1 infected or mock infected mouse spleen and vagal ganglia labeled with RNAscope in situ probes for TLR7 or Ppib (housekeeping gene) were imaged at 60x on the Zeiss Apotome Microscope. The same light intensity and exposure time was used to image H1N1 and mock infected tissue, but varied between the different tissues and probes to obtain optimal images for each tissue and probe. For the spleen, a 60x image was taken from 3 different portions from the same mouse, and for the vagal ganglia, multiple 60x images capturing the whole ganglia within a single section were obtained for each animal. Images were analyzed by ImageJ (version 1.52p, National Institutes of Health), where a color threshold was set to detect signal by the in situ probes. Each image was closely reviewed to ensure that the area detected by the set threshold and included in the analysis was true signal from an in situ probe. The area of TLR7 expression within 3 different pieces of spleen was normalized to the area of Ppib expression in a similar location in a serial section, to normalize for differences in RNA integrity between animals. For the vagal ganglia in each mouse, the total area of RNAscope signal was normalized to the total area of vagal ganglia analyzed, which included only the ganglia and not large nerve fibers passing through. Again, TLR7 expression in the vagal ganglia was normalized to Ppib expression detected in the same region of a serial section to control for differences in RNA integrity between animals.

Statistics. Comparison of mouse weights before and after infection, and cellular nitric oxide fluorescence, were analyzed by a one-way ANOVA with a Sidak post hoc test for multiple comparisons. Quantification of viral titers in the lungs and in situ hybridization labeling in the spleen and vagal ganglia of mock- and H1N1-infected mice were analyzed by a two-tailed unpaired T-test. All data was analyzed using GraphPad Prism (8.3.0, San Diego, CA). P values less than 0.05 were considered significant.

Results

TLR7 is expressed by non-neuronal cells in dorsal root and vagal ganglia

The specificity of RNA-specific mouse TLR7 probes was assessed in wild type and TLR7 knock out (KO) mice using in situ hybridization. As per previous reports [28], TLR7 was extensively expressed in wild type mouse spleens (Fig. 1A). TLR7 was not detected in spleens from TLR7 KO mice, indicating that the probe was specific for TLR7 mRNA. Expression of the housekeeping gene piptidylprolyl isomerase B (Ppib), a cyclosporine-binding protein, was detected in serial sections of both the wild type and TLR7 KO mouse spleen (Fig. 1A), confirming that RNA was present all the tissue. A negative control probe for the bacterial gene dihyrdodipicolinate reductase (DapB) showed no signal in either the wild type or TLR7 KO spleen (Fig. 1A). TLR7 expression was also detected in dorsal root (Fig. 1B) and vagal ganglia (Fig. 1C) from wild type mice and specifically localized to small cells alongside nerve cell bodies, but not within nerves.

In rare instances, a single TLR7 in situ signal was observed within a neuronal cell body (Fig. 1B, neuron labeled N*), indicating either that neuronal TLR7 expression was exceptionally uncommon or that an adjacent TLR7-expressing support cell overlapped a neuron in the Z plane of the tissue section. TLR7 was absent in dorsal root ganglia from TLR7 KO mice (Fig. 1B).

A separate, guinea pig-specific RNA probe for TLR7 similarly detected TLR7 in guinea pig spleen (Fig. 2) and in small cells located adjacent to nerve cell bodies in nodose, jugular, and dorsal root ganglia. As expected, a guinea pig-specific probe for Ppib detected RNA in serial sections throughout the ganglia, including nerve cell bodies and the negative control probe DapB was not detected, confirming that the TLR7 probe signal was not the result of background signal (Fig. 2).

TLR7 is expressed by Iba1-positive macrophages and satellite glial cells in ganglia

Guinea pig nodose and jugular ganglia sections were co-labeled with antibodies against the macrophage and satellite glial cell marker Iba-1 and against the neuronal protein PGP9.5 after performing TLR7 in situ hybridization. TLR7 colocalized exclusively with Iba1 expressing cells outside and in close proximity to neuronal cell bodies within both the nodose and jugular ganglia (Fig. 3A). TLR7 RNA expression did not overlap with the neuronal marker PGP 9.5 (Fig. 3A). These data indicate TLR7 is not expressed in sensory nerve cell bodies, but instead is expressed in non-neuronal macrophage and satellite glial support cells within ganglia.

TLR7-expressing support cells adhere to pulmonary afferents in dissociated ganglia

To further investigate TLR7 expression in guinea pig sensory ganglia, RNA was isolated from the whole dorsal root ganglia, nodose ganglia, and jugular ganglia. TLR7 RNA was detected by conventional PCR in all the ganglia (Fig. 3B). To further test whether sensory neurons that innervate the lungs express TLR7, lung-specific nerves were labeled by instilling wheat germ agglutinin (WGA) conjugated with an Alexa 555 fluorophore into the nose of anesthetized guinea pigs. After 3 days, dissociated nodose and jugular cells were sorted by flow cytometry to isolate WGA labeled (WGA+) cells (Fig. 3C). No WGA + cells were observed in the dorsal root ganglia (data not shown). TLR7 RNA was expressed in 3 out of 3 samples of WGA + cells collected from the nodose ganglia and 0 out of 3 samples of WGA + cells collected from the jugular ganglia (Fig. 3D). Cycle threshold values for TLR7 were high (e.g. CT's ranging from 33–36), indicating very low expression TLR7 expression in the WGA + cells collected from the nodose ganglia. Since macrophages and satellite glial cells express TLR7 [5, 29] and in situ hybridization analysis suggested that small cells outside of the neurons express TLR7, this same RNA was assayed for Iba1 expression to determine if macrophages and satellite glial cells were sorted alongside WGA + neurons. Iba1 RNA was expressed in 2 out of the 3 samples of WGA + cells isolated from the nodose ganglia and in 3 out of the 3 samples of WGA + cells collected from the jugular ganglia (Fig. 3E). Since neurons are not known to express Iba1, these data suggest that macrophages and satellite glial cells, which appear in

close association with neurons, failed to dissociate from the neurons and were sorted alongside WGA + neurons. Indeed, when sorted WGA + cells were labeled using in situ hybridization in culture, small TLR7-expressing support cells were present adhering to adjacent neurons (Fig. 3F). Dissociated neurons and support cells were loaded with a nitric oxide detecting fluorophore and treated with a TLR7 agonist R837 in culture. Support cells, but not neurons, increased their nitric oxide fluorescence in response to TLR7 agonist (Fig. 3G). TLR7-mediated nitric oxide release from support cells was blocked by TLR7 antagonist and by the nitric oxide synthase inhibitor L-NAME.

TLR7 expression increases during influenza A infection in mouse spleen, but not vagal ganglia

Wild type mice were inoculated with H1N1 influenza A or vehicle to determine if respiratory virus infection induces TLR7 expression, particularly in vagal neurons. Four days after inoculation, H1N1-infected mice lost significant weight (Fig. 4A) and H1N1 RNA was detected in their lung homogenates using real-time RT-PCR (Fig. 4B). Viral RNA was not present in mock infected animals. In H1N1-infected animals, TLR7 RNA expression was significantly increased in the spleen four days after infection (Fig. 4C-D). In contrast, H1N1 infection did not increase TLR7 expression in vagal ganglia (Fig. 4E-F), nor did viral infection induce TLR7 expression in nerve cells bodies (Fig. 4E). For further confirmation, the contralateral vagal ganglia from each mouse was homogenized and analyzed for TLR7 RNA expression by quantitative RT-PCR. Similar to the result obtained by the in situ hybridization assay, TLR7 RNA expression was not increased in the vagal ganglia from H1N1 infected mice (Fig. 4G). These data show that TLR7 RNA expression in the vagal ganglia is not affected by H1N1 infection.

Commercial TLR7 antibodies label small and medium sensory neurons in a TLR7-independent manner

Sections of wild type, TLR7 KO, and guinea pig dorsal root ganglia and vagal ganglia were immunolabeled with previously-cited commercial TLR7 antibodies [13, 15, 30–32]. Tissue sections from wild type and TLR7 KO mice were processed simultaneously and reacted with DAB for the same duration to ensure equal treatment. In both wild type or TLR7 knock out mice, TLR7 antibodies labeled small- to medium-sized neurons within the dorsal root ganglia (Fig. 5A **and** Fig. 6A) and nodose and jugular ganglia (Fig. 5B **and** Fig. 6B). In general, TLR7 antibody did not label larger neurons in either the dorsal root ganglia and vagal ganglia from both the wild type and knock out mice. This same pattern of staining was also observed in guinea pig dorsal root ganglia and nodose and jugular ganglia (Fig. 5C **and** Fig. 6C). Slides that did not receive primary antibody (i.e. no primary antibody control) were processed in parallel with other slides and showed no background labeling from secondary antibodies alone. Thus, although the pattern of TLR7 antibody staining appears to be specific to ganglia nerve cell bodies of a specific size, staining in both wild-type and in TLR7 KO mice clearly demonstrates that these antibodies are not specific for TLR7.

Discussion

Determining TLR7's neuromodulatory mechanisms in sensory ganglia has been complicated by conflicting reports indicating both the presence and absence of TLR7 expression by sensory nerves and by off target effects of some TLR7 agonists [13–18, 33]. As a result, whether TLR7's effects on nerve function are due to direct activation of nerves or mediated by secondary messengers released from support cells in ganglia, such as macrophages and satellite glial cells, is not clear. Several studies that show neuronal TLR7 expression have relied solely on antibody-based immunohistochemistry [13, 15, 30, 31] or have analyzed expression using PCR products from dissociated ganglia consisting of both neurons and non-neuronal support cells [13, 31]. Here, we clearly show that peri-neuronal support cells, but not sensory neurons, express TLR7 in vagal and dorsal root ganglia. We also show using immunohistochemistry that previously cited TLR7 antibodies label small and medium sized neurons in a TLR7-independent manner. These findings suggest TLR7 agonists' modulate peripheral sensory nerve function in ganglia indirectly, likely through activation of TLR7-expressing macrophages and satellite glial cells. Our results also indicate that other reports of neuronal TLR7 expression on enteric nerves [31] and trigeminal ganglia [30, 32], which were based on immunohistochemistry, should be re-examined.

Ganglia support cells, of which macrophages and satellite glial cells are some of the most common, have a key role in sensory nerve homeostasis and modulate neuronal excitability in the setting of nerve injury [34, 35]. As in other tissues, macrophages in ganglia are phagocytic cells that contribute to antigen-presentation [36, 37], whereas satellite glial cells are unique to peripheral nervous tissues, providing structural support by closely surrounding neuronal somata and directly communicating with other satellite glial cells via gap junctions [35]. Following nerve injury, neuronal mediators including nitric oxide and ATP activate macrophages and satellite glial cells [38, 39], and in turn, support cells contribute to nerve regeneration and repair [40, 41]. Activated support cells also release inflammatory cytokines TNF-alpha and IL-1beta [39], which sensitize neuronal nociceptors and increase nerve excitability to acutely enhance sensations of pain [34, 42]. Due to unknown factors in some individuals, nociceptor sensitization persists and results in disorders of chronic pain and chronic itch [43]. The factors that bias support cells and their mediators towards development of these pathologic nerve states is an area of intense interest given their potential as therapeutic targets in these conditions.

TLR7 stimulation is one mechanism by which macrophages and satellite glial cells are activated [29, 44], which may contribute sensory nerve sensitization. TLR7 agonists potentiated chloroquine-induced, but not histamine-induced scratching behavior in mice, while TLR7-deficient mice had reduced scratching, suggesting TLR7 mediates pruritis by increasing peripheral sensory nerve excitability in response to non-histaminergic stimuli [15]. Similarly, TLR7 activation enhanced withdrawal responses to painful stimuli in mice [13, 14, 16]. In both instances, direct activation of TLR7 on sensory nerves was proposed. However, our results suggest direct activation of TLR7 on neurons is unlikely since TLR7 expression was essentially absent from sensory nerve cell bodies. Only rarely was a single TLR7 in situ signal localized in a nerve, and since this signal is not robust, it is highly unlikely that neurons express TLR7. Several reasons may account for discrepancies between our results and previous studies. For one, we show that the pattern of anti-TLR7 antibody staining in small to medium-sized sensory neurons in both vagal and dorsal root ganglia, which previous studies have cited as evidence of neuronal TLR7 expression, is in fact

binding a target other than TLR7 since staining was identical in both wild-type and TLR7 knockout mice. In contrast, TLR7 situ hybridization probes show TLR7-specific staining in peri-neuronal support cells in wild type, but not in TLR7 knockout mice, and does not show staining in neurons in either WT or TLR7 knockout mice. The TLR7 RNA probe additionally labeled cells in spleen from wild-type, but not TLR7 knockout mice, providing further evidence of TLR7 probe specificity. Secondly, previous RT-PCR-based analyses tested RNA from whole ganglia and often pooled multiple ganglia together to obtain sufficient RNA, which our results show are likely to contain a variety of non-neuronal TLR7-expressing support cells. In our study, the macrophage and satellite glial cell marker Iba1 was detectable despite sorting for pulmonary-specific afferent neurons using retrograde wheat germ agglutinin labeling, indicating that closely-associated macrophages remained adherent to neurons during sorting or perhaps that macrophages acquired wheat germ agglutinin from nearby neurons, as has been reported [45]. In either case, previous RT-PCR results should be interpreted with caution given the high probability of contamination by support cell RNA. Thirdly, in many cases, the depolarizing effects of TLR7 imidazoquinoline agonists in single neurons also have well-established TLR7-independent effects on intracellular calcium, particularly at concentrations reported to induce itch [33, 46]. Finally, it is unlikely that strain- and species-specific differences account for differing results since our study and most prior studies both used mice on a C57BL/6 background and since our results using TLR7-specific RNA probes were reproducible in guinea pigs as well as mice.

In both neuronal and non-neuronal tissues, TLR7 is activated by GU-rich single-stranded RNA [1, 14]. However, unlike in other tissues, TLR7's role in the nervous system may not be primarily for antiviral immunity. For example, TLR7 was not required for viral clearance from the central nervous system in mice infected with polytropic retrovirus Fr98 despite producing an abundance of neuroinflammatory mediators including interferon gamma, TNF-alpha and CCL2 [47]. Absence of TLR7 in knockout mice also had no effect on viral replication. Our results similarly do not support a role for TLR7 in sensory ganglia during systemic influenza A infection given that TLR7 expression did not increase in ganglia support cells nor was TLR7 expression induced in neurons de novo 4 days after inoculation. While our results do not definitively exclude TLR7 activity in ganglia during infection, it is notable that TLR7 in spleen was significantly upregulated by influenza A, suggesting that TLR7 may have distinct roles in different tissues.

The full scope of TLR7's functions in the nervous system remains an open question. TLR7 has recently been shown to serve as a receptor for the endogenous microRNA Let-7b, which may help regulate microglial pruning of neurons in the central nervous system during early development in humans [48] and is elevated in neurodegenerative diseases such as Alzheimer's [49] where it may contribute to neuronal loss [11, 12]. Japanese Encephalitis Virus provoked Let7b release from neurons, causing microglial caspase activation leading to neuronal cell death [50]. In the peripheral nervous system, activated dorsal root sensory nerves released Let-7b *in vitro* and intraplantar injections of Let-7b induced pain in mice [14], suggesting microRNA's act as paracrine signals via TLR7 within sensory ganglia as well.

Our laboratory has focused on TLR7's role in pulmonary afferents given that influenza A, parainfluenza, and other respiratory viruses, which bind to TLR7, also potentiate nerve-mediated bronchoconstriction over a matter of days [19–22], and since synthetic TLR7 agonists paradoxically relax airways within minutes via release of nitric oxide [25]. TLR7 expression was also reportedly increased in severe asthma [51]. Our current results effectively exclude activation of TLR7 directly on pulmonary sensory nerves by viruses or by synthetic agonists. Whether these ligands influence nerve function indirectly via TLR7 activation on support cells, possibly via satellite cell release of nitric oxide [38], is the focus of future investigations.

Conclusion

Using species-specific TLR7 probes for in situ hybridization, we show that TLR7 is not expressed in the neurons of sensory ganglia as previously suggested, but instead in ganglia support cells including macrophages and satellite glial cells that are in close proximity to neurons. Thus, TLR7's neuromodulatory effects on peripheral sensory nerves are likely mediated indirectly through ganglia support cells. Our results also do not support a role for TLR7 in ganglia in the immune response to respiratory viral infection. TLR7's expression and function in ganglia are important considerations when designing TLR7-targeted therapeutics to treat pathologic nerve states like chronic pain.

List Of Abbreviations

DapB dihyrdodipicolinate reductase

DAPI 4',6-diamidino-2-phenylidndole

DRG dorsal root ganglia

Iba1 ionized calcium binding adaptor molecule 1

PBST phosphate buffered saline containing 0.05% Tween-20

PGP9.5 protein gene product 9.5

Ppib piptidylprolyl isomerase B

RT room temperature

RT-PCR reverse transcriptase polymerase chain reaction

$TCID_{50}$ mean tissue culture infectious dose

TLR7 toll like receptor 7

WGA wheat germ agglutinin

Declarations

Ethics Approval: Animals were treated in accordance with standards established by the United States Animal Welfare Act set forth by National Institutes of Health guidelines. The Institutional Animal Care and Use Committee at Oregon Health & Science University approved all experimental protocols.

Consent for Publication: Not applicable.

Availability of Data and Materials: The datasets generated and analyzed for this study are available from the corresponding author on reasonable request.

Competing Interests: DM declares he is a paid consultant for Pfizer, Inc., Alkermes, Inc., and Tensive Controls, Inc. MD reports he is a paid consultant for GlaxoSmithKline and AstraZeneca.

Funding: MD: Collins Foundation, GM118964 (NIH/NIGMS), HL121254 (NIH/NHLBI), American Lung Association Mountain Pacific Research Grant**.** DJ: HL144008 (NIH/NHLBI), HL113023 (NIH/NHLBI). DM: CA184324 (NIH/NCI), CA217989 (NIH/NCI).

Authors' Contributions*:* BP assisted in the design of the study, performed in situ and immunohistochemistry experiments, analyzed data, and was a major contributor to in writing the manuscript. KW assisted with immunohistochemistry experiments. MN and KM assisted with virus infection and RT-PCR experiments. DM assisted in design of the study. AF and DJ contributed to study design and manuscript preparation. MD designed the study, performed virus infection, quantified viral titers, and wrote the manuscript. All authors read, edited, and approved the final submitted manuscript.

Acknowledgements: The authors would like to acknowledge the Oregon Health & Science University Department of Comparative Medicine and Advance Light Microscopy Core.

References

1. Lund JM, Alexopoulou L, Sato A, Karow M, Adams NC, Gale NW, Iwasaki A, Flavell RA: **Recognition of single-stranded RNA viruses by Toll-like receptor 7.***Proc Natl Acad Sci U S A* 2004, **101:**5598-5603.
2. Li Q, Yan Y, Liu J, Huang X, Zhang X, Kirschning C, Xu HC, Lang PA, Dittmer U, Zhang E, Lu M: **Toll-Like Receptor 7 Activation Enhances CD8+ T Cell Effector Functions by Promoting Cellular Glycolysis.***Front Immunol* 2019, **10:**2191.
3. Hanten JA, Vasilakos JP, Riter CL, Neys L, Lipson KE, Alkan SS, Birmachu W: **Comparison of human B cell activation by TLR7 and TLR9 agonists.***BMC Immunol* 2008, **9:**39.
4. Drake MG, Bivins-Smith ER, Proskocil BJ, Nie Z, Scott GD, Lee JJ, Lee NA, Fryer AD, Jacoby DB: **Human and Mouse Eosinophils Have Antiviral Activity against Parainfluenza Virus.***Am J Respir Cell Mol Biol* 2016, **55:**387-394.
5. Gantier MP, Tong S, Behlke MA, Xu D, Phipps S, Foster PS, Williams BR: **TLR7 is involved in sequence-specific sensing of single-stranded RNAs in human macrophages.***J Immunol* 2008, **180:**2117-2124.

6. Eng HL, Hsu YY, Lin TM: **Differences in TLR7/8 activation between monocytes and macrophages.***Biochem Biophys Res Commun* 2018, **497:**319-325.
7. Roberts AW, Lee BL, Deguine J, John S, Shlomchik MJ, Barton GM: **Tissue-Resident Macrophages Are Locally Programmed for Silent Clearance of Apoptotic Cells.***Immunity* 2017, **47:**913-927 e916.
8. Grassin-Delyle S, Abrial C, Salvator H, Brollo M, Naline E, Devillier P: **The Role of Toll-Like Receptors in the Production of Cytokines by Human Lung Macrophages.***J Innate Immun* 2020, **12:**63-73.
9. Akira S, Takeda K: **Toll-like receptor signalling.***Nat Rev Immunol* 2004, **4:**499-511.
10. Lehmann SM, Kruger C, Park B, Derkow K, Rosenberger K, Baumgart J, Trimbuch T, Eom G, Hinz M, Kaul D, et al: **An unconventional role for miRNA: let-7 activates Toll-like receptor 7 and causes neurodegeneration.***Nat Neurosci* 2012, **15:**827-835.
11. Lehmann SM, Rosenberger K, Kruger C, Habbel P, Derkow K, Kaul D, Rybak A, Brandt C, Schott E, Wulczyn FG, Lehnardt S: **Extracellularly delivered single-stranded viral RNA causes neurodegeneration dependent on TLR7.***J Immunol* 2012, **189:**1448-1458.
12. Liu HY, Hong YF, Huang CM, Chen CY, Huang TN, Hsueh YP: **TLR7 negatively regulates dendrite outgrowth through the Myd88-c-Fos-IL-6 pathway.***J Neurosci* 2013, **33:**11479-11493.
13. He L, Han G, Wu S, Du S, Zhang Y, Liu W, Jiang B, Zhang L, Xia S, Jia S, et al: **Toll-like receptor 7 contributes to neuropathic pain by activating NF-kappaB in primary sensory neurons.***Brain Behav Immun* 2020, **87:**840-851.
14. Park CK, Xu ZZ, Berta T, Han Q, Chen G, Liu XJ, Ji RR: **Extracellular microRNAs activate nociceptor neurons to elicit pain via TLR7 and TRPA1.***Neuron* 2014, **82:**47-54.
15. Liu T, Xu ZZ, Park CK, Berta T, Ji RR: **Toll-like receptor 7 mediates pruritus.***Nat Neurosci* 2010, **13:**1460-1462.
16. Qi J, Buzas K, Fan H, Cohen JI, Wang K, Mont E, Klinman D, Oppenheim JJ, Howard OM: **Painful pathways induced by TLR stimulation of dorsal root ganglion neurons.***J Immunol* 2011, **186:**6417-6426.
17. Goethals S, Ydens E, Timmerman V, Janssens S: **Toll-like receptor expression in the peripheral nerve.***Glia* 2010, **58:**1701-1709.
18. Wang J, Kollarik M, Ru F, Sun H, McNeil B, Dong X, Stephens G, Korolevich S, Brohawn P, Kolbeck R, Undem B: **Distinct and common expression of receptors for inflammatory mediators in vagal nodose versus jugular capsaicin-sensitive/TRPV1-positive neurons detected by low input RNA sequencing.***PLoS One* 2017, **12:**e0185985.
19. Lee AM, Fryer AD, van Rooijen N, Jacoby DB: **Role of macrophages in virus-induced airway hyperresponsiveness and neuronal M2 muscarinic receptor dysfunction.***Am J Physiol Lung Cell Mol Physiol* 2004, **286:**L1255-1259.
20. Drake MG, Evans SE, Dickey BF, Fryer AD, Jacoby DB: **Toll-like receptor-2/6 and Toll-like receptor-9 agonists suppress viral replication but not airway hyperreactivity in guinea pigs.***Am J Respir Cell Mol Biol* 2013, **48:**790-796.

21. Rynko AE, Fryer AD, Jacoby DB: **Interleukin-1beta mediates virus-induced m2 muscarinic receptor dysfunction and airway hyperreactivity.***Am J Respir Cell Mol Biol* 2014, **51:**494-501.
22. Nie Z, Scott GD, Weis PD, Itakura A, Fryer AD, Jacoby DB: **Role of TNF-alpha in virus-induced airway hyperresponsiveness and neuronal M(2) muscarinic receptor dysfunction.***Br J Pharmacol* 2011, **164:**444-452.
23. Empey DW, Laitinen LA, Jacobs L, Gold WM, Nadel JA: **Mechanisms of bronchial hyperreactivity in normal subjects after upper respiratory tract infection.***Am Rev Respir Dis* 1976, **113:**131-139.
24. Johnston SL, Pattemore PK, Sanderson G, Smith S, Lampe F, Josephs L, Symington P, O'Toole S, Myint SH, Tyrrell DA, et al.: **Community study of role of viral infections in exacerbations of asthma in 9-11 year old children.***BMJ* 1995, **310:**1225-1229.
25. Drake MG, Scott GD, Proskocil BJ, Fryer AD, Jacoby DB, Kaufman EH: **Toll-like receptor 7 rapidly relaxes human airways.***Am J Respir Crit Care Med* 2013, **188:**664-672.
26. Kaufman EH, Fryer AD, Jacoby DB: **Toll-like receptor 7 agonists are potent and rapid bronchodilators in guinea pigs.***J Allergy Clin Immunol* 2011, **127:**462-469.
27. Dubuis E, Grace M, Wortley MA, Birrell MA, Belvisi MG: **Harvesting, isolation, and functional assessment of primary vagal ganglia cells.***Curr Protoc Pharmacol* 2013, **62:**12 15 11-12 15 27.
28. Nishimura M, Naito S: **Tissue-specific mRNA expression profiles of human toll-like receptors and related genes.***Biol Pharm Bull* 2005, **28:**886-892.
29. Mitterreiter JG, Ouwendijk WJD, van Velzen M, van Nierop GP, Osterhaus A, Verjans G: **Satellite glial cells in human trigeminal ganglia have a broad expression of functional Toll-like receptors.***Eur J Immunol* 2017, **47:**1181-1187.
30. Helley MP, Abate W, Jackson SK, Bennett JH, Thompson SW: **The expression of Toll-like receptor 4, 7 and co-receptors in neurochemical sub-populations of rat trigeminal ganglion sensory neurons.***Neuroscience* 2015, **310:**686-698.
31. Barajon I, Serrao G, Arnaboldi F, Opizzi E, Ripamonti G, Balsari A, Rumio C: **Toll-like receptors 3, 4, and 7 are expressed in the enteric nervous system and dorsal root ganglia.***J Histochem Cytochem* 2009, **57:**1013-1023.
32. Larsson O, Tengroth L, Xu Y, Uddman R, Kumlien Georen S, Cardell LO: **Substance P represents a novel first-line defense mechanism in the nose.***J Allergy Clin Immunol* 2018, **141:**128-136 e123.
33. Kim SJ, Park GH, Kim D, Lee J, Min H, Wall E, Lee CJ, Simon MI, Lee SJ, Han SK: **Analysis of cellular and behavioral responses to imiquimod reveals a unique itch pathway in transient receptor potential vanilloid 1 (TRPV1)-expressing neurons.***Proc Natl Acad Sci U S A* 2011, **108:**3371-3376.
34. Ji RR, Chamessian A, Zhang YQ: **Pain regulation by non-neuronal cells and inflammation.***Science* 2016, **354:**572-577.
35. Hanani M, Spray DC: **Emerging importance of satellite glia in nervous system function and dysfunction.***Nat Rev Neurosci* 2020, **21:**485-498.

36. Wang PL, Yim AKY, Kim KW, Avey D, Czepielewski RS, Colonna M, Milbrandt J, Randolph GJ: **Peripheral nerve resident macrophages share tissue-specific programming and features of activated microglia.***Nat Commun* 2020, **11:**2552.
37. Ural BB, Yeung ST, Damani-Yokota P, Devlin JC, de Vries M, Vera-Licona P, Samji T, Sawai CM, Jang G, Perez OA, et al: **Identification of a nerve-associated, lung-resident interstitial macrophage subset with distinct localization and immunoregulatory properties.***Sci Immunol* 2020, **5**.
38. Belzer V, Hanani M: **Nitric oxide as a messenger between neurons and satellite glial cells in dorsal root ganglia.***Glia* 2019, **67:**1296-1307.
39. Zhang X, Chen Y, Wang C, Huang LY: **Neuronal somatic ATP release triggers neuron-satellite glial cell communication in dorsal root ganglia.***Proc Natl Acad Sci U S A* 2007, **104:**9864-9869.
40. Gallaher ZR, Ryu V, Herzog T, Ritter RC, Czaja K: **Changes in microglial activation within the hindbrain, nodose ganglia, and the spinal cord following subdiaphragmatic vagotomy.***Neurosci Lett* 2012, **513:**31-36.
41. Kwon MJ, Kim J, Shin H, Jeong SR, Kang YM, Choi JY, Hwang DH, Kim BG: **Contribution of macrophages to enhanced regenerative capacity of dorsal root ganglia sensory neurons by conditioning injury.***J Neurosci* 2013, **33:**15095-15108.
42. Zelenka M, Schafers M, Sommer C: **Intraneural injection of interleukin-1beta and tumor necrosis factor-alpha into rat sciatic nerve at physiological doses induces signs of neuropathic pain.***Pain* 2005, **116:**257-263.
43. Yu X, Liu H, Hamel KA, Morvan MG, Yu S, Leff J, Guan Z, Braz JM, Basbaum AI: **Dorsal root ganglion macrophages contribute to both the initiation and persistence of neuropathic pain.***Nat Commun* 2020, **11:**264.
44. Celhar T, Pereira-Lopes S, Thornhill SI, Lee HY, Dhillon MK, Poidinger M, Connolly JE, Lim LH, Biswas SK, Fairhurst AM: **TLR7 and TLR9 ligands regulate antigen presentation by macrophages.***Int Immunol* 2016, **28:**223-232.
45. Yakura T, Miki T, Warita K, Ohta K-i, Suzuki S, Matsumoto Y, Liu J-Q, Tamai M, Takeuchi1 Y: **Satellite glial cells in the nodose ganglion of the rat vagus nerve: Morphological alterations of microglial cells.***Biomedical Research* 2013, **24:**1-6.
46. Hwang H, Min H, Kim D, Yu SW, Jung SJ, Choi SY, Lee SJ: **Imiquimod induces a Toll-like receptor 7-independent increase in intracellular calcium via IP(3) receptor activation.***Biochem Biophys Res Commun* 2014, **450:**875-879.
47. Lewis SD, Butchi NB, Khaleduzzaman M, Morgan TW, Du M, Pourciau S, Baker DG, Akira S, Peterson KE: **Toll-like receptor 7 is not necessary for retroviral neuropathogenesis but does contribute to virus-induced neuroinflammation.***J Neurovirol* 2008, **14:**492-502.
48. Paolicelli RC, Bolasco G, Pagani F, Maggi L, Scianni M, Panzanelli P, Giustetto M, Ferreira TA, Guiducci E, Dumas L, et al: **Synaptic pruning by microglia is necessary for normal brain development.***Science* 2011, **333:**1456-1458.

49. Simon E, Obst J, Gomez-Nicola D: **The Evolving Dialogue of Microglia and Neurons in Alzheimer's Disease: Microglia as Necessary Transducers of Pathology.***Neuroscience* 2019, **405:**24-34.
50. Mukherjee S, Akbar I, Kumari B, Vrati S, Basu A, Banerjee A: **Japanese Encephalitis Virus-induced let-7a/b interacted with the NOTCH-TLR7 pathway in microglia and facilitated neuronal death via caspase activation.***J Neurochem* 2019, **149:**518-534.
51. Shikhagaie MM, Andersson CK, Mori M, Kortekaas Krohn I, Bergqvist A, Dahl R, Ekblad E, Hoffmann HJ, Bjermer L, Erjefalt JS: **Mapping of TLR5 and TLR7 in central and distal human airways and identification of reduced TLR expression in severe asthma.***Clin Exp Allergy* 2014, **44:**184-196.

Figures

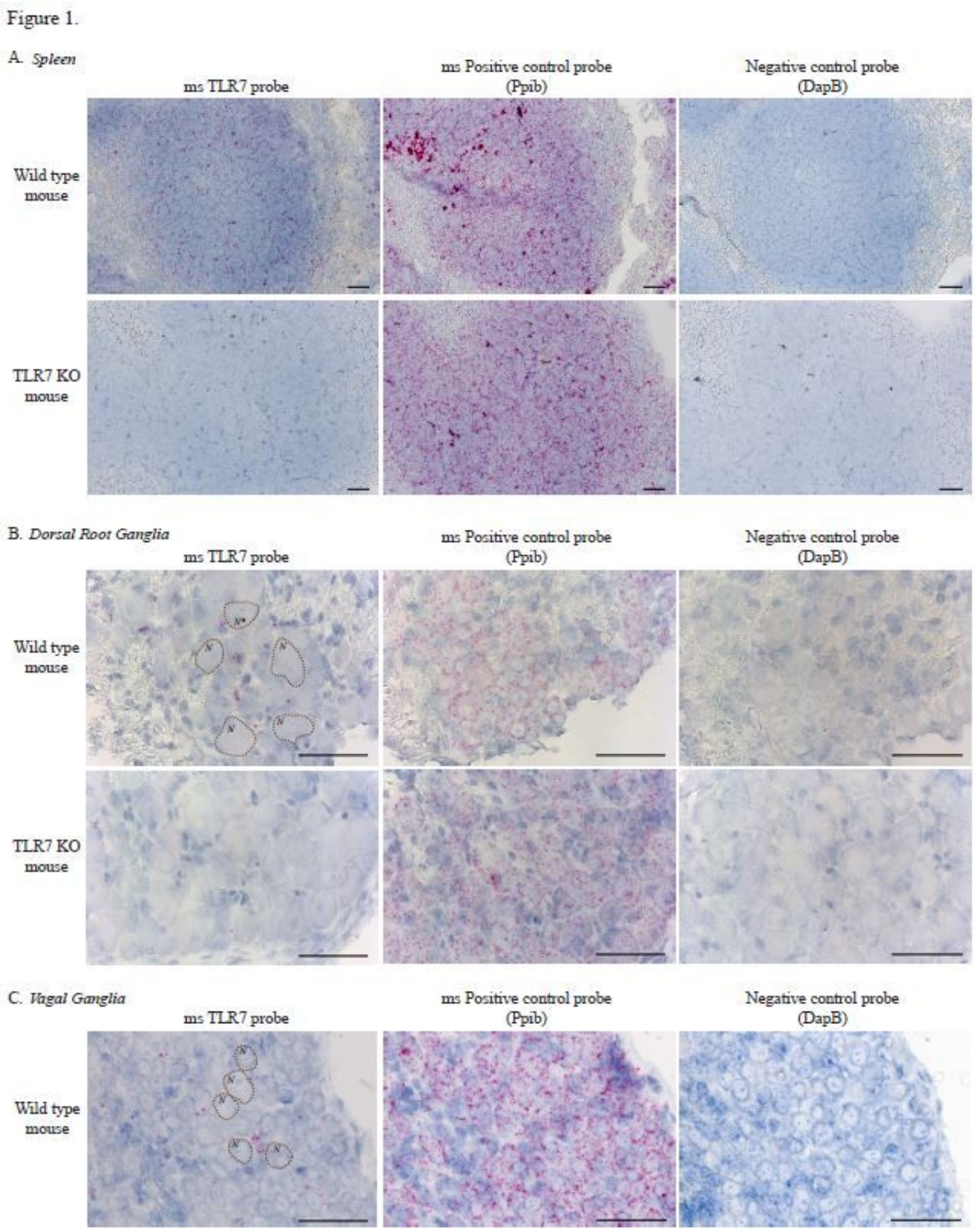

Figure 1

TLR7 is expressed by peri-neuronal support cells in mouse sensory ganglia. (A) Mouse-specific TLR7 in situ hybridization probe was tested in wild type and TLR7 KO mouse spleen. TLR7 (pink) was detected in the spleen from wild type mice, but not in TLR7 KO mice, confirming the specificity of the probe. The housekeeping gene Ppib (pink) was used as positive control to confirm RNA integrity, and an in situ probe for the bacterial protein DapB served as a negative control to assess in situ hybridization background

signal. (B) TLR7 in situ probes labeled small cells located in close proximity to neuronal cell bodies (N) within dorsal root ganglia in wild type mice. Rarely, a single TLR7 in situ probe signal could be found in a neuronal cell body (N*). TLR7 was absent in dorsal root ganglia from TLR7 knockout mice. Representative neuronal cell bodies are outlined within the ganglia. (C) TLR7 in situ probes similarly labeled small cells adjacent to sensory neuron cell bodies (N) in vagal ganglia from a wild type mouse. Blue = hematoxylin nuclear stain in all images. N = 4, representative images shown. Scale bar = 50 μm

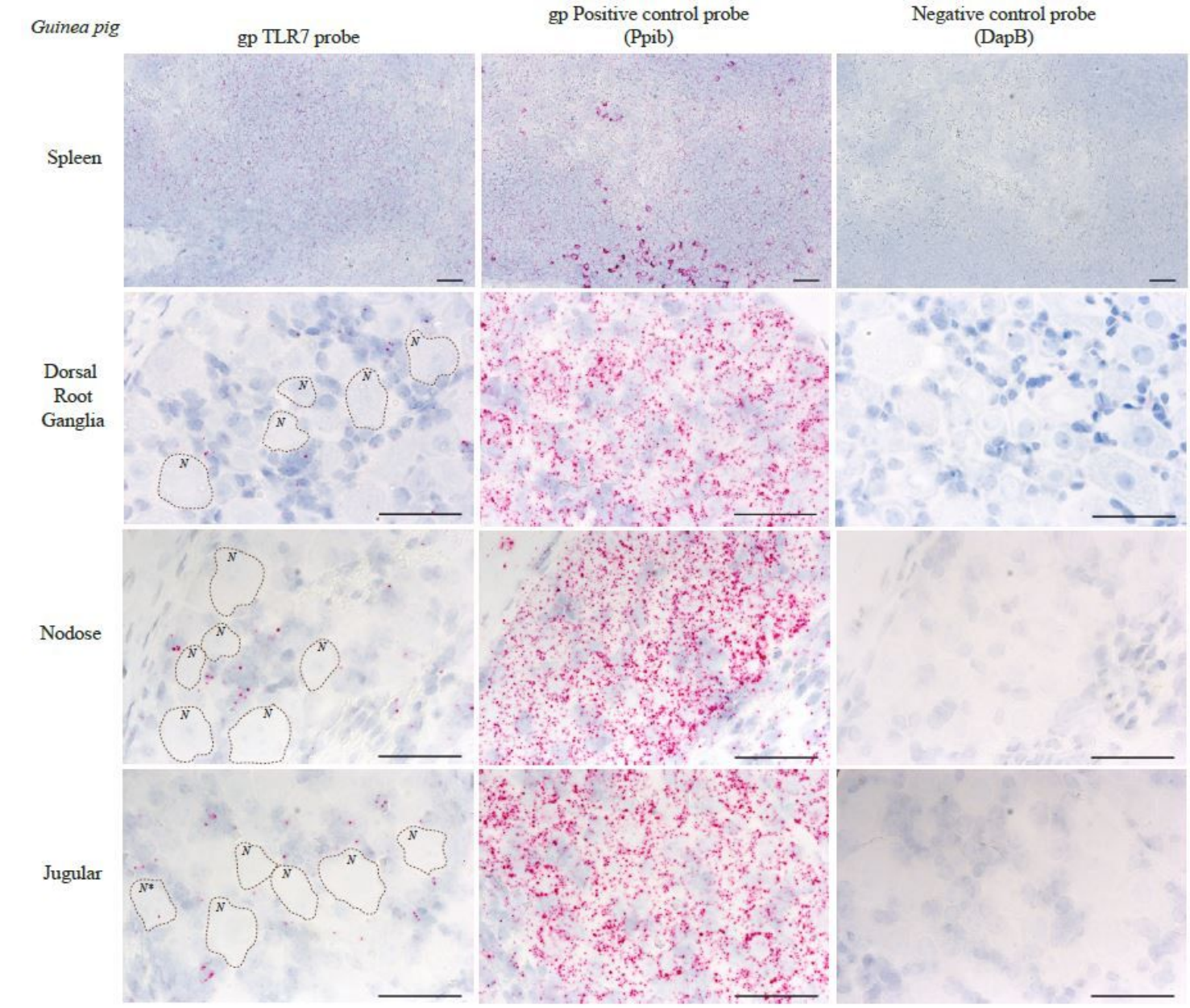

Figure 2

TLR7 is expressed by support cells in guinea pig vagal and dorsal root ganglia. Guinea pig-specific in situ hybridization probe detected TLR7 (pink) in small cells located outside neuronal cell bodies (N) in dorsal root ganglia, and in nodose and jugular ganglia, which comprise the vagal ganglia. The housekeeping gene Ppib (pink) was also detected in spleen and ganglia, while the negative control probe (DapB)

showed no signal as expected. Rarely, a single TLR7 in situ probe signal could be found in a neuronal cell body (N*). Representative neuronal cell bodies (N) within ganglia are outlined in the image. Blue = hematoxylin nuclear stain in all images. N = 4, representative images shown. Scale bar = 50 μm

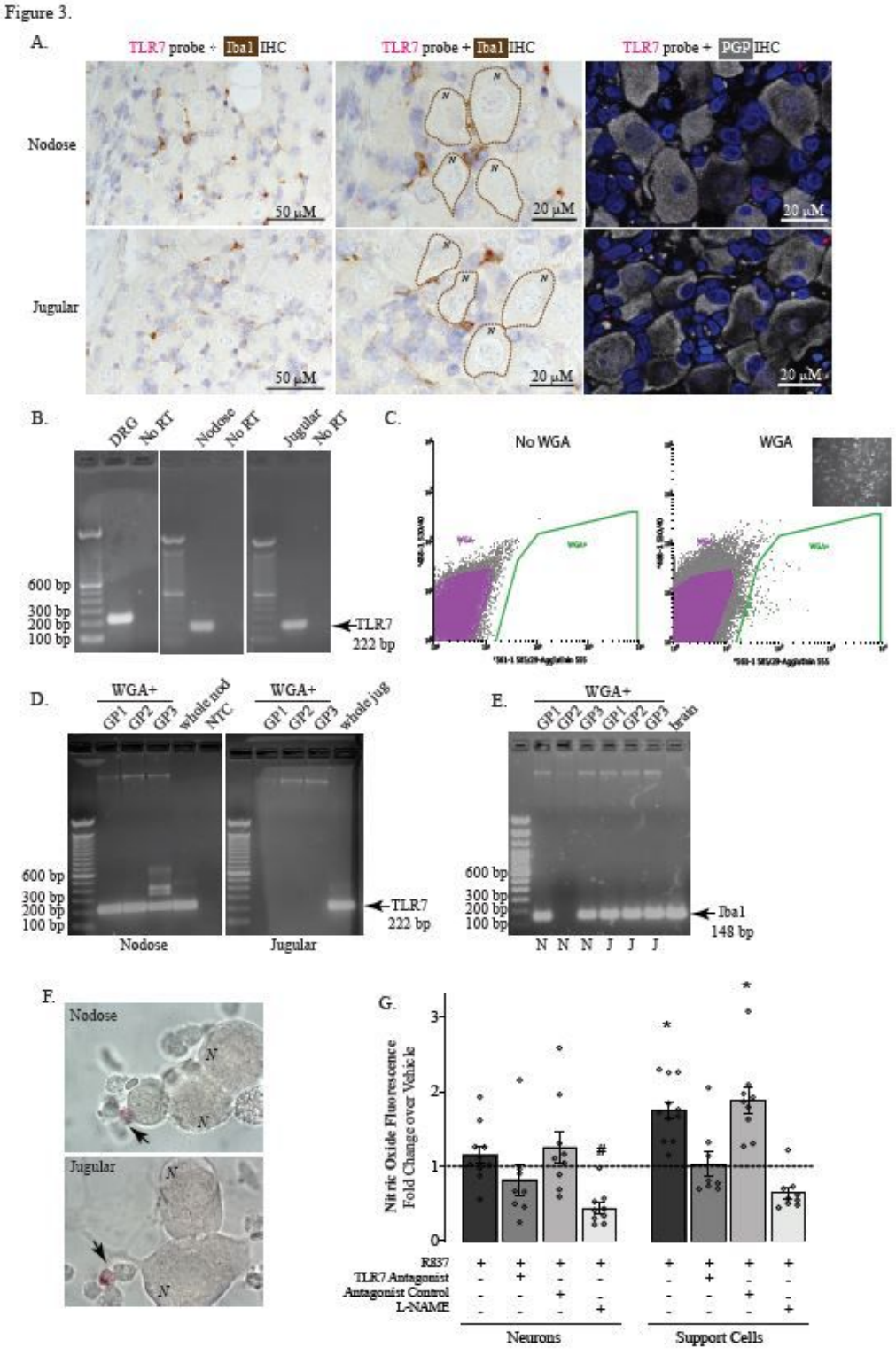

Figure 3

TLR7 is co-expressed in Iba1 expressing cells within the nodose and jugular ganglia. (A) Guinea pig nodose and jugular ganglia were co-labeled with TLR7 in situ hybridization probes and antibodies for

colorimetric and fluorescent immunohistochemistry. TLR7 RNA (pink) colocalized with cells expressing the macrophage marker Iba1 (brown), but not with the pan neuronal marker PGP (gray). N = neurons (selected neurons are labeled in the images). Blue = hematoxylin or dapi nuclear stain, Representative images shown, N = 4. (B) Using RT-PCR, TLR7 RNA was expressed in guinea pig whole dorsal root ganglia (DRG), nodose ganglia, and jugular ganglia. Representative agarose gels (DRG N = 3 animals, nodose and jugular N = 4 animals each). No RT = No reverse transcriptase control. (C-E) Alexa 555-conjuaged wheat germ agglutinin (WGA) labeled lung-specific nerves in the nodose and jugular ganglia in guinea pigs. Control animals received PBS (no WGA). Flow cytometry isolated WGA expressing (WGA+) cells. (C) A representative flow cytometry sort selecting for WGA+ cells (outlined green area) from cells that do not express WGA (WGA-) from a dissociated nodose ganglia. The inset picture is a whole mount image (10x) of a nodose labeled with WGA before dissociation. (D) TLR7 RNA was detected in WGA+ cells sorted from dissociated nodose, but not from the jugular ganglia in 3 guinea pigs (GP1-3). Whole nodose (whole nod) and whole jugular (whole jug) RNA = positive controls, NTC = no template control. (E) The same RNA WGA+ cells sorted from dissociated nodose and jugular ganglia also expressed Iba1 RNA. Brain RNA = positive control, N = Nodose, J = Jugular. (F) TLR7 in situ probes detected TLR7 (pink, arrows) in small cells from dissociated nodose and jugular ganglia. N = neurons. (G) Cultured neurons and support cells from dissociated ganglia were loaded with the nitric oxide detecting fluorophore and treated with the TLR7 agonist R837. Support cells, but not neurons, produced nitric oxide in response to TLR7 agonist. N = 8-10 replicates. Each replicate represents the average from 10-20 individual cells.

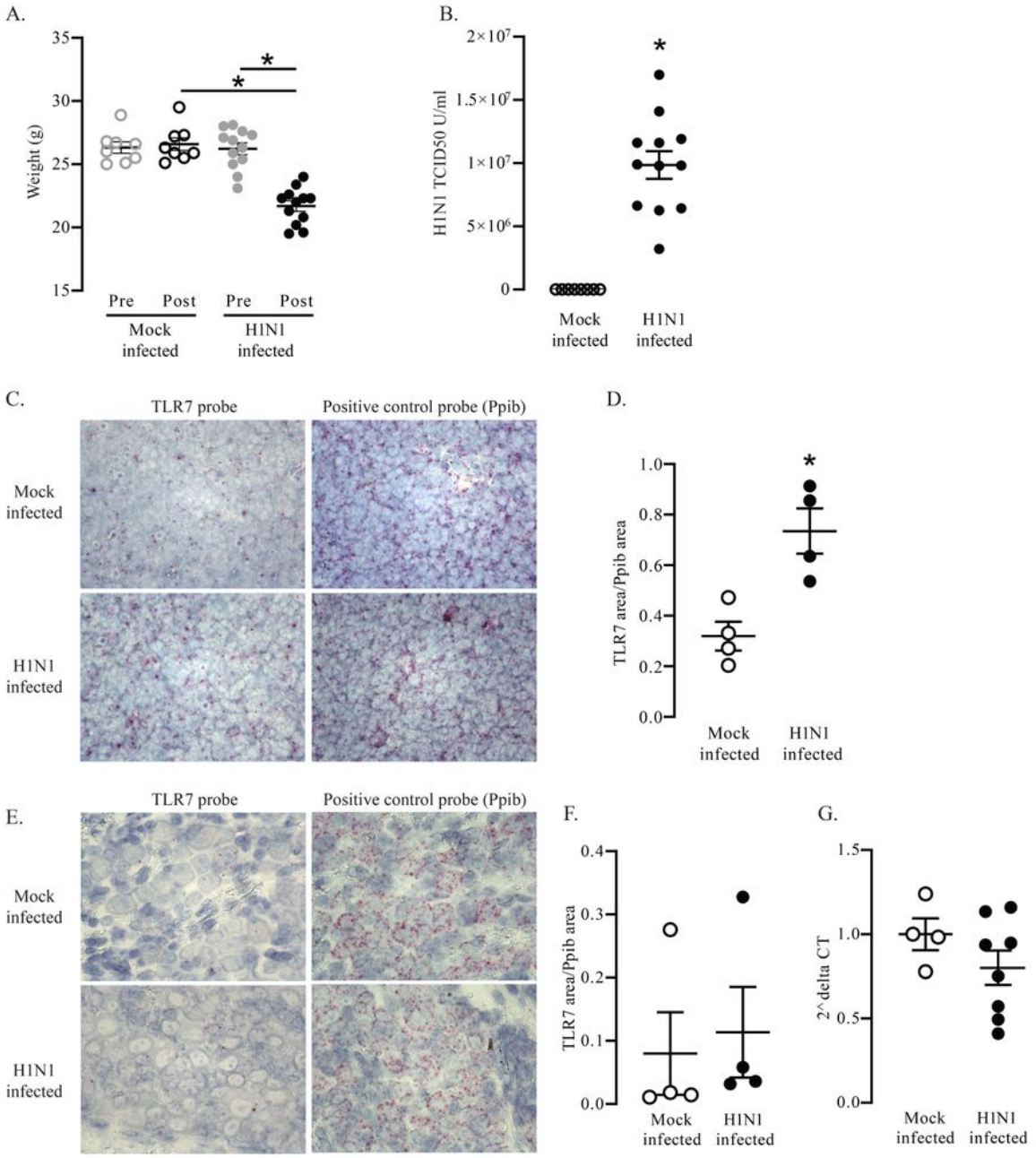

Figure 4

TLR7 RNA expression in mouse spleen and vagal ganglia after H1N1 infection. (A) Wild type mice were weighed before (pre) and four days after (post) inoculation with H1N1 (H1N1 infected) or PBS vehicle (mock infected). Body weights were significantly reduced in H1N1 infected mice. (B) H1N1 viral titers were quantified from lung tissue by real time RT-PCR four days after inoculation. H1N1 viral RNA was present only in the mice inoculated with H1N1. N = 8-12. (C) Sections of spleen were labeled with either

the TLR7 or the housekeeping gene Ppib in situ hybridization probes (pink, representative images). Blue = hematoxylin nuclear stain. (D) TLR7 RNA was quantified and normalized to housekeeping RNA Ppib expression. H1N1 infection significantly increased TLR7 RNA expression in mouse spleen. N = 4. (E) Sections of the vagal ganglia were labeled with either TLR7 or the house keeping gene Ppib in situ hybridization probes (pink, representative images). Blue = hematoxylin nuclear stain. (F) TLR7 RNA expression was quantified and normalized to Ppib expression. H1N1 infection did not affect TLR7 expression in mice vagal ganglia. (G) Similarly, in the contralateral ganglia, TLR7 RNA expression, quantified by real time RT-PCR, was not affected by H1N1 infection. N = 4. *$p < 0.05$

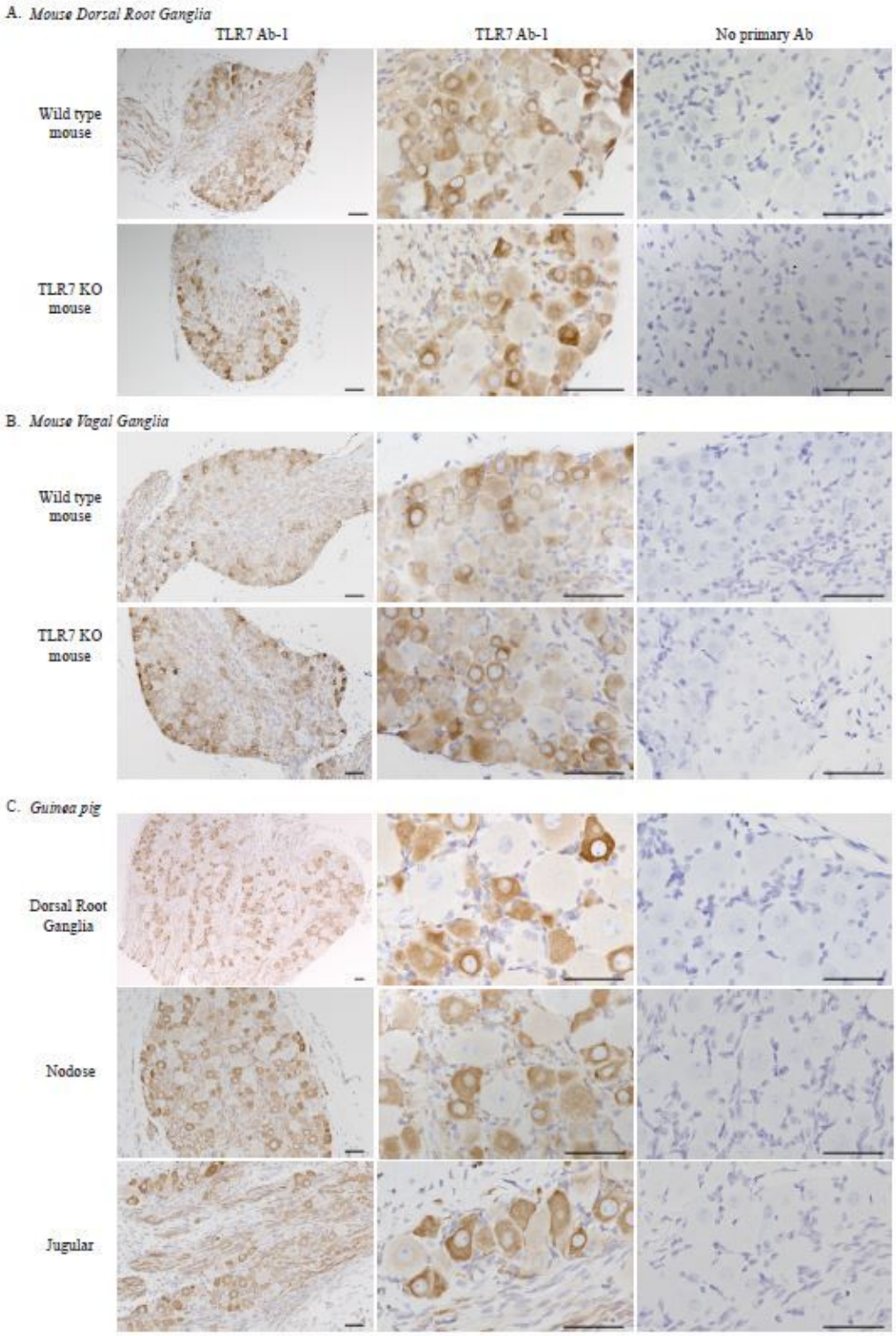

Figure 5

Immunohistochemistry with a TLR7 antibody reveals TLR-independent labeling of small and medium-sized sensory neurons. Mouse dorsal root ganglia and vagal ganglia were collected from wild type mice and TLR7 knock out (KO) mice and paraffin sections were processed for immunohistochemistry. A TLR7 antibody (brown, TLR7 Ab-1, Novus) labeled small-to-medium-sized neurons in (A) dorsal root ganglia and (B) vagal ganglia in both wild type and TLR7 KO mice, indicating that this antibody is not specific for

TLR7. (C) An identical staining pattern for TLR7 (brown) was detected in guinea pig dorsal root ganglia and nodose and jugular ganglia. Scale bar = 50 μm. Blue = hematoxylin nuclear stain. N = 4, representative images shown.

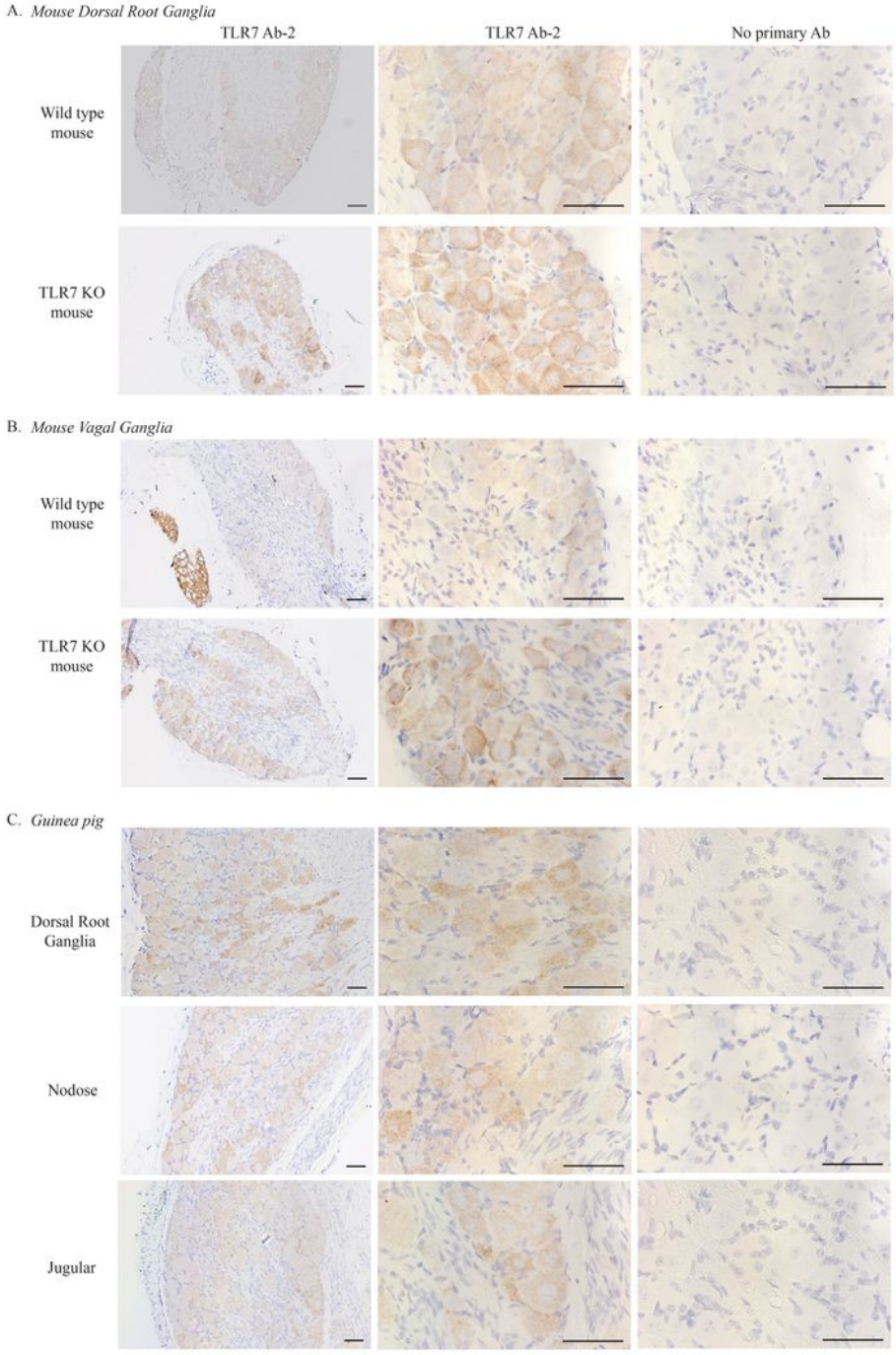

Figure 6

Immunohistochemistry using a second TLR7 antibody similarly shows TLR7-independent sensory neuron labeling. A second commercially-available TLR7 antibody (brown, TLR7 Ab-2, Abcam) labeled small-to-

medium-sized neurons in the (A) dorsal root ganglia and (B) vagal ganglia in both wild type and TLR7 KO mice, and in (C) guinea pig dorsal root, nodose, and jugular ganglia. The presence of TLR7 staining in TLR7 knockout animals indicates that this antibody is not specific for TLR7 in neuronal tissues. Scale bar = 50 μm. Blue = hematoxylin nuclear stain. N = 4; representative images shown.